

Dynamics of the ions in Liquid Argon Detectors and electron signal quenching

Luciano Romero, Roberto Santorelli,* and Bárbara Montes

Centro de Investigaciones Energéticas,

Medioambientales y Tecnológicas (CIEMAT) Av. Complutense 40, 28040 Madrid, Spain

(Dated: June 7, 2022)

Abstract

A study of the dynamics of the positive charges in liquid argon has been carried out in the context of the future massive time projection chambers proposed for dark matter and neutrino physics. The ions spend considerably longer times in the active volume with respect to the electrons given their small mobility coefficient in liquid. The space charge can be additionally increased by the injection in the target volume of the ions produced by electron multiplying devices located in a gas phase above the liquid. The impact of the positive current on the uniformity of the field has been evaluated as well as the probability of the charge signal quenching due to the electron-ion recombination along the drift. The results show a potential concern for the operation of massive detectors with drift of many meters when located on surface.

Keywords: Argon, TPC, noble gases, space charge, neutrino, dark matter

* Corresponding author. E-mail address: roberto.santorelli@ciemat.es.

CONTENTS

I. Introduction	2
II. Dynamic of the ions at the interface gas/liquid	4
III. Electron/ion recombination and drift field distortion	6
A. Particle currents and drift field equations	8
IV. Results and discussion	10
V. Conclusions	17
Acknowledgments	17
Appendices	17
A. Calculation of the field lines	17
B. Cathode voltage calculation	20
References	20

I. INTRODUCTION

The liquid argon (LAr) technology has been widely used during the recent years in several fields ranging from neutrino physics [1–3] to direct dark matter searches [4–6]. In particular a massive liquid argon time projection chamber (LAr-TPC) is the preferred option for the next generation of neutrino observatories recently proposed [7], given its particle identification and low energy threshold capabilities in large active volumes [8].

Particle interactions in argon produce simultaneously excitation and ionization of the atoms, generating, at the same time, VUV photons and ion/electron pairs. In a typical LAr-TPC, photon sensors are used to detect the prompt scintillation light, while a constant electric field \vec{E}_d drifts the electrons to the anode. Charge measurement can be done through the collection of the electrons on thin wires placed directly in liquid [9] or, for double phase liquid-vapor detectors, through the extraction of the electrons from the liquid phase and

their multiplication in the gas region placed above the sensitive volume [10]. In the last case a Townsend avalanche can be induced through high electric fields, producing an amplified signal proportional to the number of primary electrons extracted from the liquid.

The direct charge readout through the wires placed in a single phase chamber has the advantage of an overall simplified detector design. However experiments foreseeing drift up to 20 m have been recently proposed [11–14], which require a considerable technological effort maintaining a level of contamination of less than 60 ppt of O₂ equivalent [15] (electron half life > 5 ms [16]), in order to reduce the impact of the electron quenching by electronegative impurities contaminating the LAr bulk. The amplification in gas makes possible to detect smaller charge signals, thus allowing to reach a lower energy threshold or, equivalently, to foresee a longer drift distance with respect to a single phase detector.

The positive and negative charges, produced by the particle interactions in liquid argon, drift to the cathode and the anode respectively following the same field lines, although the former have a drift speed which is six orders of magnitude lower than that of the latter, $v_i \ll v_e$ [17, 18]. As a consequence, the ions spend longer time in liquid before they get collected on the cathode and neutralized, thus the positive charge density is much larger than that of the electrons ($\rho_i \gg \rho_e$). The effect can be particularly relevant in case of a readout foreseeing the charge amplification, such that other ions are further created by the avalanche in gas. It has to be considered the possibility that those ions drift back to the cathode crossing the gas-liquid interface, thus, for large amplification factors, ρ_i can be increased by the charge created in gas. The space charge can locally modify the amplitude of the electric field, the drift lines and the velocity of the electrons produced in liquid, leading to a displacement in the reconstructed position of the ionization signal. Additionally, the positive density ρ_i can be relevant enough such that the probability of a “secondary electron/ion recombination”, different than the primary columnar recombination, has to be considered between the electrons produced by particle interactions in liquid and the ion current. The effect can cause an additional signal loss, with a probability dependent on the electron drift path, that could resemble the charge quenching given by the electronegative impurities in the active volume.

The dynamic of the positive charge density produced by the cosmic rays and by the ³⁹Ar contamination in natural argon has been investigated in the present article, evaluating its impact on the electron signal in massive argon detectors. The study is particularly relevant

for the new generation of neutrino experiments foreseeing drift paths of many meters.

II. DYNAMIC OF THE IONS AT THE INTERFACE GAS/LIQUID

The electrons, produced in liquid, drift to the anode and are then extracted and accelerated in gas, with the production of a Townsend avalanche. It is possible that the Ar ions, produced at the same time, scatter onto field lines not ending in the liquid surface, however, given the low diffusion of the ions in gas relatively to the typical size of the amplification region, a non-negligible fraction of those can drift back to the liquid interface along the same field lines of the electrons. When the distance between the ion and the liquid-vapor interface is greater than several angstroms, the liquid can be treated as a continuum, thus an approximated description of the dynamic can be obtained solving a boundary condition problem between different dielectrics with the mirror charge method in a single dimension [19]. Accordingly, a point like charge q in a medium with permittivity ϵ placed at the interface with another medium with permittivity ϵ' produces a mirror charge $q' = -q \cdot (\epsilon' - \epsilon)/(\epsilon' + \epsilon)$. Taking into account that the relative permittivity is $\epsilon_{LAr} = 1.5$ for liquid argon and $\epsilon_{GAr} = 1$ for argon vapor, the corresponding potential energy for an ion placed at a distance $d > 0$ from the liquid-vapor interface is function of the inverse of the distance from the surface [20, 21]:

$$V_{LAr}(d) = \frac{q^2}{16\pi\epsilon_0\epsilon_{LAr}} \left(\frac{\epsilon_{LAr} - \epsilon_{GAr}}{\epsilon_{LAr} + \epsilon_{GAr}} \right) \frac{1}{d} + c_{LAr} \equiv \frac{A_{LAr}}{d} + c_{LAr}, \quad (1)$$

$$V_{GAr}(d) = \frac{q^2}{16\pi\epsilon_0\epsilon_{GAr}} \left(\frac{\epsilon_{GAr} - \epsilon_{LAr}}{\epsilon_{LAr} + \epsilon_{GAr}} \right) \frac{1}{d} + c_{GAr} \equiv \frac{A_{GAr}}{d} + c_{GAr}, \quad (2)$$

and it is depicted in Fig. 1, where the integration constants c_{GAr} and c_{LAr} account for the potential energy of the ion when it is far from the interface (see Eq. 3).

Classically, the potential is infinite at $d = 0$, thus it has been sometimes assumed that the barrier can preclude the ions from reaching the liquid phase [22], although that is true only if the charge can be approximated as point-like. Considering dimensions of the order of 1 Å, as it is the case for the ionized atomic or molecular states whose formation is typical in noble gases [8], the mirror approximation is no longer valid. As the ion approaches the interface, it induces a displacement of the charge in the liquid that reduces the potential energy. The effective potential should decrease monotonically as the ion plunge into the

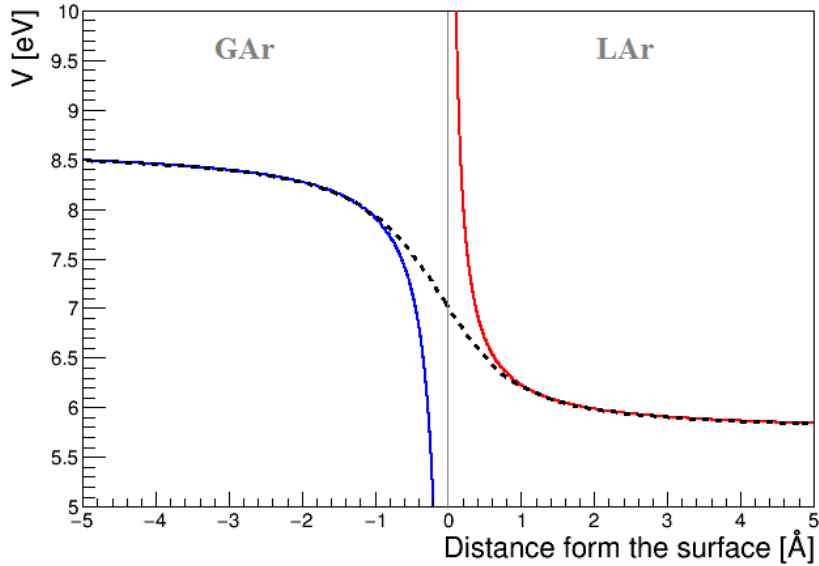


FIG. 1. Potential energy (solid lines) at the liquid (right-red) / vapor (left-blue) interface in the mirror charge approximation and possible effective potential energy (dashed line, see text for details).

liquid, following a sigmoidal shape (Fig. 1 - dashed line), thus the problem is reduced to a finite classical potential barrier.

At the same time, the crossing of the liquid/gas interface is energetically favored. Considering the ion as an uniformly charged sphere of radius a , its potential energy far from the surface can be expressed as:

$$V = \frac{3}{5} \frac{q^2}{4\pi\epsilon a}. \quad (3)$$

Taking into account that a is of the order of ≈ 1 Å, the ≈ 2.9 eV difference between the potential energies at the interface allows, in principle, the injection of the ions into the liquid¹, thus the possibility that a large fraction of the positive charge produced in gas enters the liquid phase cannot be discarded.

For the present study it is irrelevant what kind of charge amplification device is used: we introduce the ion gain G_I defined as the number of positive ions injected into the liquid for each electron extracted. That factor is proportional to the electron amplification G through

¹ According with the model presented, the difference between liquid and gas for the ions is one order of magnitude bigger than that for the electrons, 0.21 eV [22].

a constant β ($\beta < 1$) which takes into account the average loss of the positive charge in gas² as well as the efficiency to pass the liquid-gas interface. If the amplification factor G_I is large enough, the positive charge density ρ_i in liquid can be widely increased by the secondary ions.

III. ELECTRON/ION RECOMBINATION AND DRIFT FIELD DISTORTION

We consider an LAr-TPC with an axial geometry and the l axis perpendicular to the surface of the liquid. The drift field \vec{E}_d in liquid is along l , with the anode at the origin ($l = 0$) and the cathode at a positive distance L . In the following calculation we assume that the detector is wide enough such that the transverse coordinate y is not relevant for the discussion and the \vec{E}_d is constant in any transverse section of the detector.

In the limit of a null ion current, the drift field is constant and it is equal to the cathode voltage divided by the total drift length L . On the contrary, the ion cloud makes the drift field to change with l , and it is minimum at the anode and maximum at the cathode. The cathode voltage necessary to obtain a given field has to take into account the ion current, and it can be calculated integrating the drift field expression as function of l .

Additionally, it has to be considered the possibility that an ion recombines along the drift with a free electron produced by the particle interactions in liquid, thus causing a quenching effect of the charge signal similarly to the one given by electronegative impurities. In order to evaluate the probability of that “secondary” recombination, different than the primary columnar recombination, we define the cross section S_{CS} as the transverse area whose crossing field lines end on one ion. The section should be far enough from the ion such that the ion field is negligible compared to the drift field. At the same time, all the lines emerging from the ion cross that section. Fig. 2 shows the field paths approaching an ion positioned at $(0,0)$, which has a negligible size at the micron scale, in case of $E_d = 1$ kV/cm (see appendix A for the detailed calculation). The dashed line is the envelope of all the field lines ending on the ion.

The total number of field lines emerging from the ion, q/ϵ , is equal to the number of lines

² The value of β depends on the geometry and the field configuration of the charge amplifying device.

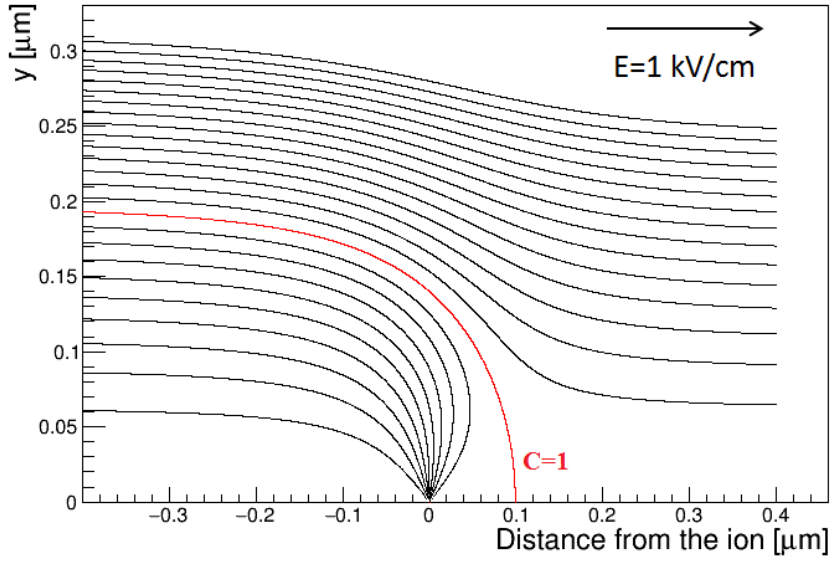


FIG. 2. Configuration of the drift field lines near an ion for 1 kV/cm. The red line, obtained for $C = 1$ (see appendix A), is the envelope of the path ending on the ion.

traversing the cross section, $E_d \cdot S_{CS}$, therefore:

$$S_{CS} = \frac{q}{\epsilon E_d}, \quad (4)$$

where q is the elementary charge, ϵ the absolute permittivity of the liquid argon and E_d the magnitude of the drift field. For a typical E_d value of 1 kV/cm, $S_{CS} = 1.2 \cdot 10^{-7} \text{ mm}^2$ is much larger than the ion dimensions, thus the sum of the S_{CS} for the overall ion cloud can be macroscopic and the contribution of the recombination cannot be neglected.

We define the ion and electron fluxes as follows:

$$j_i(l) = v_i(l)\rho_i(l), \quad j_e(l) = v_e(l)\rho_e(l), \quad (5)$$

where $\rho(l)$ and $v(l)$ are the particle density and velocity respectively at distance l , being the last one related to the drift field through the mobility coefficient μ in liquid argon:

$$v_i(l) = \mu_i E_d(l), \quad v_e(l) = \mu_e E_d(l). \quad (6)$$

Considering a typical drift field of $E_d = 1 \text{ kV/cm}$, the experimental value for electron velocity is $v_e \approx 2 \text{ mm}/\mu\text{s}$ [17]. On the other hand, the ion mobility, measured in steady state by subtracting the liquid motion, is $\mu_i \approx 2 \cdot 10^{-4} \text{ cm}^2 \text{ V}^{-1}\text{s}^{-1}$ [18]. Even considering

the more conservative values of $\mu_i \approx 1.6 \cdot 10^{-3} \text{ cm}^2 \text{ V}^{-1} \text{s}^{-1}$ [23] the expected ion velocity is $v_i \approx 1.6 \cdot 10^{-5} \text{ mm}/\mu\text{s}$, which is five orders of magnitude lower than that of the electrons.

The recombination rate, $r(l)$, in $\text{m}^{-3} \text{s}^{-1}$, is given by the ion density multiplied by the flux of the electrons and by the cross section:

$$r(l) = \rho_i(l) j_e(l) S_{CS}(l). \quad (7)$$

Substituting ρ_i , v_i and S_{CS} from Eq. 5, 6 and 4 we obtain:

$$r(l) = \frac{j_i(l) j_e(l)}{v_i(l)} \frac{q}{\epsilon E_d(l)} = j_i(l) j_e(l) \frac{q}{\mu_i \epsilon E_d^2(l)}, \quad (8)$$

which allows to determine the charge signal loss in liquid knowing the currents and the drift field.

A. Particle currents and drift field equations

Environmental radioactivity, ^{39}Ar decay and cosmic muons continuously produce interactions within the liquid argon bulk. All those sources are assumed to be uniformly distributed in the volume, so we can introduce a constant ionization rate, h , defined as the average number of free ion-electron pairs, produced by particle interactions in liquid per unit of time and volume, which escape the primary recombination.

In a stationary state the variation of the density of ions and electrons in any point should be null, therefore:

$$0 = h - r(l) - \frac{dj_i(l)}{dl}, \quad 0 = h - r(l) + \frac{dj_e(l)}{dl}. \quad (9)$$

The electron current diminishes with the axial distance, l , therefore the quantity dj_e/dl is negative. Replacing in Eq. 9 the recombination rate given by expression 8, we get:

$$\frac{dj_i(l)}{dl} + j_i(l) j_e(l) \frac{q}{\mu_i \epsilon E_d^2(l)} = h, \quad \frac{dj_e(l)}{dl} - j_i(l) j_e(l) \frac{q}{\mu_i \epsilon E_d^2(l)} = -h. \quad (10)$$

On the other hand, the variation of the drift field, that we assume parallel to the detector axis, is determined by the charge density:

$$-q \rho_e(l) + q \rho_i(l) = \epsilon \frac{dE_d(l)}{dl}. \quad (11)$$

Since the ions spend considerably longer time in liquid before they get collected on the cathode, the positive charge density is much larger than that of the electrons. Being $\rho_i \gg \rho_e$

we can disregard ρ_e in Eq. 11. Considering the expression of the ion density from Eq. 5, and using expression 6, we have:

$$j_i(l) = \frac{\epsilon v_i(l)}{q} \frac{dE_d(l)}{dl} = \frac{\epsilon \mu_i E_d(l)}{q} \frac{dE_d(l)}{dl} = \frac{1}{2} \frac{\epsilon \mu_i}{q} \frac{dE_d^2(l)}{dl}. \quad (12)$$

Equations 10 and 12 are three coupled differential equations with three functions (j_i , j_e and E_d) and one variable l . The argument of those equations can be simplified introducing the function

$$f(l) = \frac{\epsilon \mu_i}{q} E_d^2(l), \quad (13)$$

then the 3 coupled linear equations stand:

$$\frac{dj_i(l)}{dl} + \frac{j_i(l) j_e(l)}{f(l)} = h, \quad \frac{dj_e(l)}{dl} - \frac{j_i(l) j_e(l)}{f(l)} = -h, \quad j_i(l) = \frac{1}{2} \frac{df(l)}{dl}. \quad (14)$$

The three boundary conditions, which allow to get a particular solution of the equations, can be obtained taking the electric field at the anode as parameter, and considering that the electron current at the cathode is null and the ion current at the anode is given by the electron current multiplied by the ion gain:

$$E_d(0) = E_A. \quad (15)$$

$$j_e(L) = 0, \quad (16)$$

$$j_i(0) = G_I j_e(0), \quad (17)$$

The system of equations given by 14 can be solved numerically for any particular detector. In order to get an approximated solution we consider as negligible the impact of the recombination in the ion current equation. That is the case since $\rho_i \gg \rho_e$ even at low or null G_I values, given the several orders of magnitude lower drift speed of the ions with respect to the electrons. Accordingly the recombination is disregarded from the first equation of 14:

$$\frac{dj_i(l)}{dl} = h \rightarrow j_i(l) = h l + j_i(0), \quad (18)$$

however it has to be taken into account for the electrons, so the second equation of 14 still stands. From the third equation of 14 and using equations 13, 15 and 18 we have:

$$f(l) = 2 \int_0^l j_i(l) dl = h l^2 + 2 j_i(0) l + f_0, \quad f_0 = f(0) = \frac{\epsilon \mu_i}{q} E_A^2. \quad (19)$$

Thus, taking into account Eq. 13, the drift field as a function of l can be written as:

$$E_d(l) = \sqrt{\frac{q}{\epsilon\mu_i}(h l^2 + 2 j_i(0) l) + E_A^2}, \quad (20)$$

and it can be calculated knowing the ion gain, the minimum field and the electron current at the anode.

The second equation of 14 can be written using 18 and 19 as:

$$\frac{d j_e(l)}{d l} - \frac{(h l + j_i(0))}{h l^2 + 2 j_i(0) l + f_0} j_e(l) = -h. \quad (21)$$

Considering the boundary condition of a null electron current at the cathode (Eq. 16), the linear differential equation can be solved analytically:

$$j_e(l) = -h F(l) \ln \left(\frac{l + j_i(0)/h + F(l)}{L + j_i(0)/h + F(L)} \right), \quad (22)$$

where

$$F(l) = \sqrt{l^2 + \frac{2 j_i(0)}{h} l + \frac{f_0}{h}}. \quad (23)$$

The electron current at the anode can be obtained calculating numerically $j_i(0)$ with Eq. 22 taking into account Eq. 17.

IV. RESULTS AND DISCUSSION

We can evaluate the effective drift field in a LAr-TPC, including the space charge effects, and the electron quenching probability considering the average ionization produced in the argon target by the ^{39}Ar decay and by the cosmic muons. Other contributions given, for example, by the natural radioactivity, the Rn decay or the material contamination, are considered negligible.

In an underground facility the dominant contribution to the charge production is typically given by the ^{39}Ar decay, a β emitter with a Q-value of 565 keV whose activity in natural argon is ≈ 1 Bq/kg [24], or, for liquid argon, ≈ 1400 Bq/m³. We can assume that the mean energy deposited per decay in the active volume is approximately one third of the total Q-value. Considering that the accepted value for the average energy required to form an ion-electron pair in liquid argon is $W = 23.6$ eV [25], a ^{39}Ar decay produces in average $\approx 8 \cdot 10^3$ pairs, therefore the ionization rate h_0 due to ^{39}Ar is $\approx 1.1 \cdot 10^7$ pairs/(m³s).

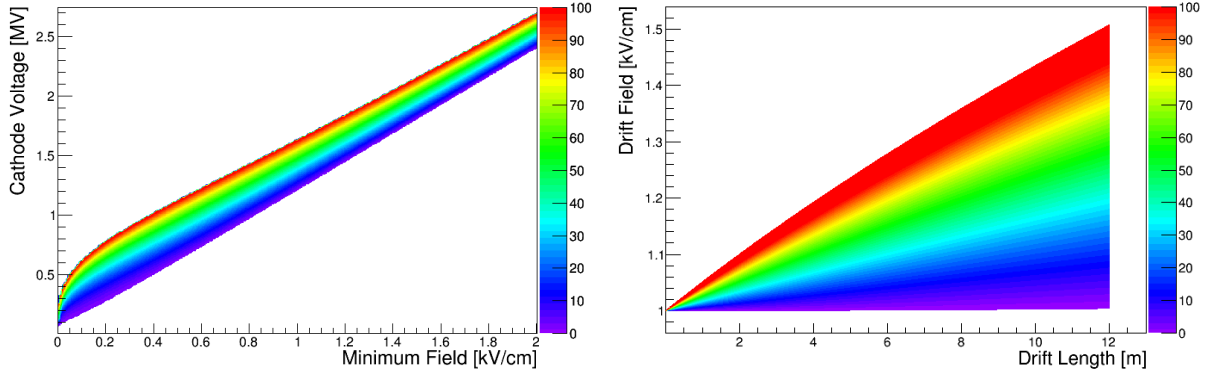


FIG. 3. Underground case: cathode voltage as function of the minimum drift field E_A , for different ion gains (color scale) in case of a dual phase 12 m LAr detector (*left*). Variation of the field inside the same detector assuming a field at the anode of 1 kV/cm for different ion gains (*right*).

The primary recombination of the electrons with the parent ions is function of the drift field and it is usually approximated with the so-called Birks law³ $h = \frac{h_0}{1+k_E/E_d}$ [26], which gives the average free charge constantly produced in liquid by the ^{39}Ar decays (see Eq. 9). The constant k_E has been experimentally measured and it is equal to 0.53 ± 0.04 kV/cm [27].

In case the detector is located on surface, the contribution to the total ionization produced in the detector is mainly given by muons. Their flux at sea level is reported to be 168 muons/(m²s) [28]. Considering that most of the muons are at their minimum ionizing energy, the energy loss in argon as function of the density is:

$$\frac{dE}{dl} \approx 1.5 \frac{\text{MeV cm}^2}{\text{g}}, \quad (24)$$

which gives an average deposited energy $dE/dl = 210$ MeV/m per muon or 35 GeV/(m³s) in liquid argon. Assuming the same W-value as before, the ion production rate is therefore: $h_0 = 1.5 \cdot 10^9$ pairs/(m³s), two orders of magnitude bigger than the one from the ^{39}Ar decay.

The positive charge density modifies the electric field in such a way that it is minimum at the anode and maximum at the cathode. We can calculate the field variation and the cathode voltage needed to produce a field E_A by integrating Eq. 20 between 0 and L (see appendix B for the detailed calculation).

³ We conservatively considered the minimal drift field or field at the anode $E_A = E_d$.

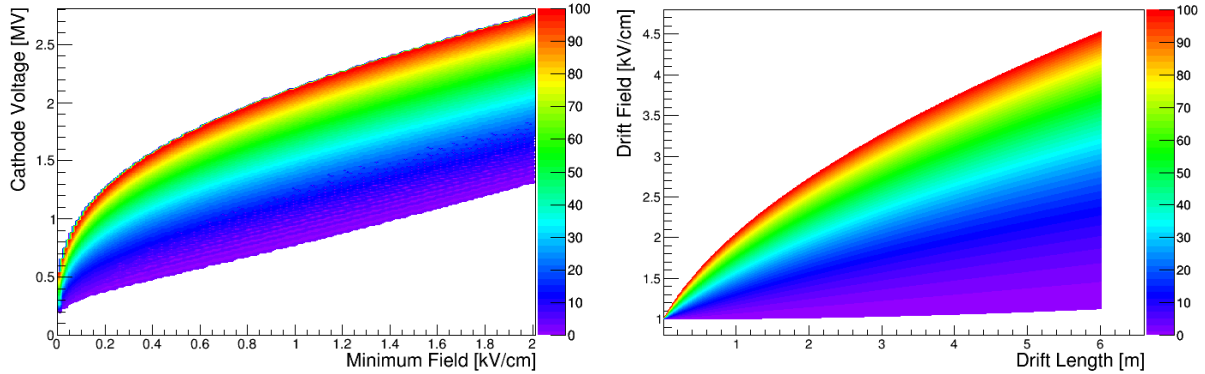


FIG. 4. Surface case: cathode voltage as function of the minimum drift field E_A , for different ion gains (color scale) in case of a dual phase 6 m LAr detector (*left*). Variation of the field inside the same detector assuming a field at the anode of 1 kV/cm for different ion gains (*right*).

Fig. 3–*left* shows the cathodic voltage needed to produce a given field at the anode for a 12 m detector placed in an underground laboratory. According with the calculations, an increase up to 50% in the nominal cathode voltage without space charge effects is necessary in order to keep the desired field at the anode. The corresponding field variation between anode and cathode is shown in Fig. 3–*right* for different ion gains. Variation of the order of 1 - 2% are expected without charge amplification on such drift lengths.

Fig. 4–*left* shows similar plots for a 6 m detector placed on surface. Cathode voltages well within the megavolts range are required in order to be able to produce a minimum field of 1 kV/cm for ion gains $G_I \gtrsim 10$, while at 600 kV only half of the nominal field, obtained without considering the ion flux, is produced at the anode in such conditions. In case of $G_I \approx 100$, voltages of the order of 2 MV are necessary to have a minimum field of 1 kV/cm inside the detector with a corresponding field at the cathode of more than 4 kV/cm. The field variation inside the detector is shown in Fig. 4–*right*. Maximum fields of the order of twice E_A are produced at the cathode for $G_I > 10$, evidencing the important non-uniformity of the field inside the detector. Even in case of $G_I = 0$, differences of the order of 10% are expected between the field at the anode and the cathode because of the primary ionization produced by the cosmic rays in liquid.

The quenching of the charge given by the electron-ion recombination along the drift can be calculated considering the probability $P(l)$ that an electron created at depth l reaches

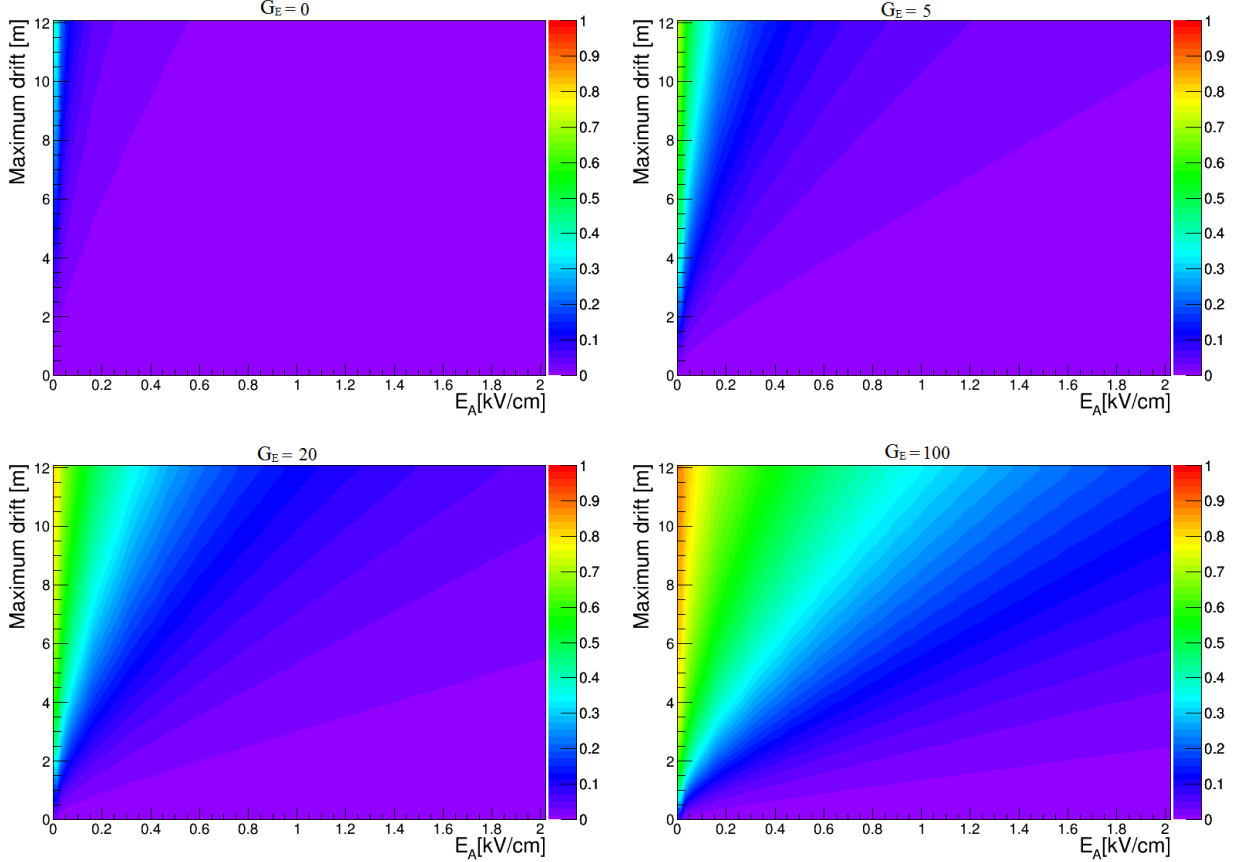


FIG. 5. Underground case: Maximum recombination probability (electrons generated at the cathode level) as function of the total drift length L and the anode field E_A , considering $G_I = 0$ (top-left), $G_I = 5$ (top-right), $G_I = 20$ (bottom-left) and $G_I = 100$ (bottom-right).

the anode. That probability is equal to the fraction of the surface $S(l)$ spanned by the field lines ending in the anode with respect to the total transverse area $S(0)$ and it is minimal for $l = L$ and one for $l = 0$. Since the number of field lines ($E \cdot S$) is conserved all along the detector depth, $E(0) \cdot S(0) = E(l) \cdot S(l)$, we obtain from Eq. 20:

$$P(l) = \frac{S(l)}{S(0)} = \frac{E(0)}{E(l)} = \frac{E_A}{\sqrt{\frac{q}{\epsilon\mu_i} (hl^2 + 2j_i(0)l) + E_A^2}}, \quad (25)$$

whose solution can be calculated knowing the constant ionization rate h , the field at the anode E_A and the ion gain G_I .

Eq. 25 has been solved for a detector placed underground considering drift lengths up to 12 m and anode fields up to 2 kV/cm. The maximum charge quenching, evaluated considering the recombination probability of the electrons produced at distance L from the

anode, is plotted in Fig. 5 as function of the drift length and field, assuming $G_I = 0$, $G_I = 5$, $G_I = 20$ and $G_I = 100$. Without charge amplification the recombination is practically negligible unless very low fields ($\lesssim 0.3$ kV/cm) and long drift distances (≈ 10 m) are foreseen. At a typical field of ≈ 1 kV/cm we can expect relatively small charge signal losses ($\leq 10\%$) for a few meters drifts and ion gains of the order of some tens, at the same time, if G_I is of the order of 100, more than 20% of the charge signal created at the cathode level is quenched after 6 m drift and more than 50% after 12 m.

Eq. 25 has been also solved for a detector placed on surface considering the same ion gains and field values as the underground case, and the corresponding secondary recombination probability is plotted in Fig. 6 for drift lengths up to 6 m. At a typical field of ≈ 1 kV/cm a measurable value for the recombination ($\approx 5\%$) is obtained in case of a single phase detector ($G_I = 0$) placed on surface with maximum drifts of 2 – 3 meters. We can expect charge signal losses $\leq 10\%$ only for a couple of meters drifts and ion gains of the order of 5 – 10, while for $G_I \geq 20$ and $L \geq 2$ m nearly half of the charge is expected to recombine. In case of G_I of the order of 100, the largest fraction of the charge created near the cathode is quenched in liquid, even at higher field or smaller drift distance.

We calculated the average charge quenching by the ion current in liquid, assuming a constant ionization rate with the interactions uniformly distributed in the active volume. In order to calculate the electron/ion recombination on an event by event basis, it has to be taken into account that specific areas with much higher ion current and field distortion compared to the calculated average values can be locally produced inside the active volume. While the uniform and constant current approximation is nicely valid for an underground detector, where the ion cloud is given by a large number of a few μm ^{39}Ar decays, the ionization paths produced in a detector placed on surface by the cosmic rays are nearly vertical tracks with length comparable to the maximum drift L . In this case, an important ion flux will be localized around the muon direction and, depending on the detector length and the ion velocity, it can last for several minutes after the muon interaction, locally blinding the detector.

At the same time, the present discussion has been carried out considering the liquid argon volume in a steady state, although the convection motion given by the temperature gradient inside the detector and the liquid recirculation necessary to keep the required argon purity have to be considered. Given the relatively fast drift time of the electrons

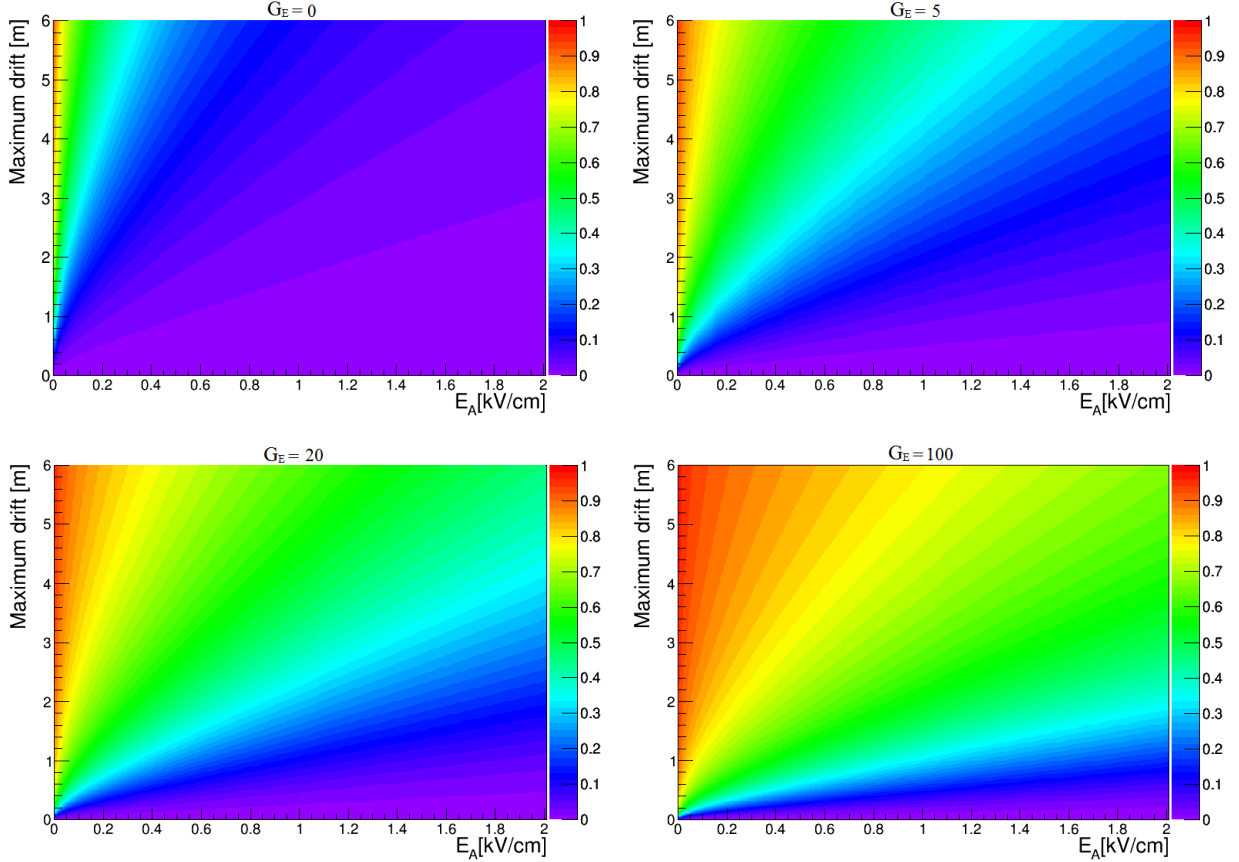


FIG. 6. Surface case: Maximum recombination probability (electrons generated at the cathode level) as function of the total drift length L and the anode field E_A , considering $G_I = 0$ (top-left), $G_I = 5$ (top-right), $G_I = 20$ (bottom-left) and $G_I = 100$ (bottom-right).

($v_e \approx 2 \text{ mm}/\mu\text{s}$ [17]), their drift is not significantly affected by the liquid motion, however, that could be the case for the six orders of magnitude slower ions. Even if only an extremely powerful recirculation flow (several tens of m^3/hour) could produce an overall motion barely comparable with the typical drift speed of the ions, the convection flows, which have been evaluated to be in the range of mm/s [10], can be comparable with the ion drift velocity and, hence, change their effective mobility.

Recent results from the analysis of the ICARUS data, taken during the commission on surface in 2001, evidenced the bending of the muon tracks reconstructed inside the T600 module [23] likely given by space charge induced electric field distortions. The small value of such effect ($\approx 3 \text{ mm}$ maximum) is consistent with the relatively short drift distance (1.5 m)

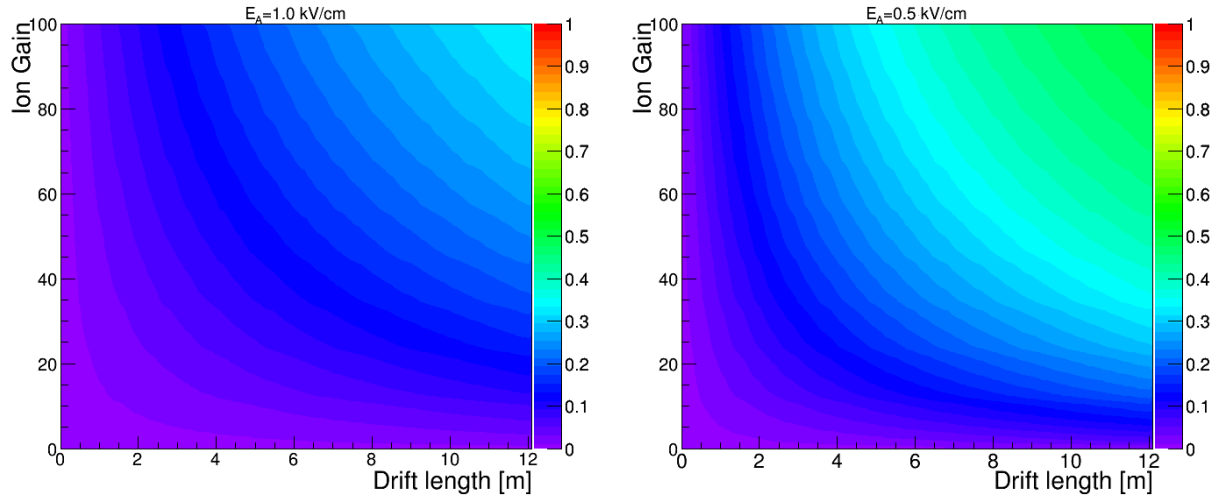


FIG. 7. Underground case: recombination probability (color scale) as function of the ion gain G_I and drift length l for a $L = 12 \text{ m}$ detector, in case of $E_A = 1.0 \text{ kV/cm}$ (left) and $E_A = 0.5 \text{ kV/cm}$ (right).

of the detector. Other experiments based on LAr-TPCs, with the drift of a few meters, presented additional evidences of space charge effects [29, 30], however no indications of a possible charge quenching by electron/ion recombination has been ever reported. According to our calculation, a few % maximum signal loss is expected, in average, considering a detector located on surface with drift fields of $0.5 - 1 \text{ kV/cm}$, $G_I = 0$ and drift length up to $\approx 3 \text{ m}$.

The Deep Underground Neutrino Experiment (DUNE) is specially relevant in this context and it can provide a fundamental proof to fully evidence the field distortion and the secondary recombination produced by the ion current in liquid. Particularly, the double phase LAr-TPC, with $L = 12 \text{ m}$ maximum drift length and the charge amplification [31], should be characterized by a measurable electron signal reduction even at small values of G_I . In Fig. 7 the secondary recombination probability is shown as function of the drift length l for different ion gains, in case of $E_A = 1.0 \text{ kV/cm}$ and $E_A = 0.5 \text{ kV/cm}$. In the first case, more than 10 % charge quenching is expected in a large section of the detector, even considering relatively small ion amplifications ($G_I \gtrsim 5$). At the same time, much larger recombination probabilities, up to 50 %, are expected at lower drift fields.

V. CONCLUSIONS

The small mobility coefficient of the positive ions in a liquid argon time projection chamber ensures that they spend considerably longer time in the active volume with respect to the electrons, thus space charge effects can be originated by the positive charge accumulation. In a double phase detector with electron signal amplification, the effect can be increased by the injection in the liquid of the ions produced by the avalanche in gas. We evaluated the impact of the ion current on the uniformity of the drift field and the probability of the charge signal quenching as function of the drift length due to the electron-ion recombination. According to our calculation, the average signal loss in a single phase underground detector is below 1% unless very long drifts ($\gtrsim 5$ m) and relatively low fields (< 0.5 kV/cm) are foreseen. Depending on the charge amplification factor in gas, a relevant effect can be detected in a double phase underground chamber. Finally the results show a potential concern for the operation of massive detectors with drift of many meters and charge amplification when operated on surface.

ACKNOWLEDGMENTS

The research has been funded by the Spanish Ministry of Economy and Competitiveness (MINECO) through the grant FPA2015-70657P. The authors were also supported by the “Unidad de Excelencia Mara de Maeztu: CIEMAT - Física de partículas” through the grant MDM-2015-0509.

Appendices

A. CALCULATION OF THE FIELD LINES

We consider a cylindrical symmetry with an arbitrary plane containing the axis and the origin. The section of the flux tubes with the plane gives the field lines, $r(\varphi)$. The coordinate system is defined such that the x axis corresponds to the field direction, and s is the arc length with arbitrary origin (see Fig. 8). Due to the cylindrical symmetry, we will only consider the half-plane with positive coordinates.

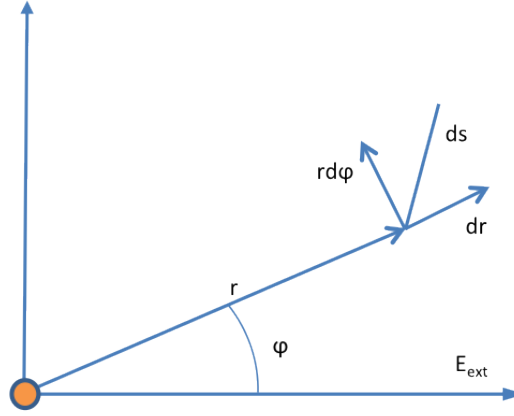


FIG. 8. Coordinate system with the ion in the origin and the external electric field in the direction of the x axis.

The external electric field in polar coordinates is expressed as follows:

$$\vec{E}_{ext} = \begin{pmatrix} E_{ext} \cos\varphi \\ -E_{ext} \sin\varphi \end{pmatrix}. \quad (26)$$

The total electric field, which takes into account the external field and the ion field is written as

$$\vec{E} = \vec{E}_{ion} + \vec{E}_{ext} = \frac{q\vec{r}}{4\pi\epsilon r^3} + \vec{E}_{ext} = \begin{pmatrix} \frac{q}{4\pi\epsilon r^2} + E_{ext} \cos\varphi \\ -E_{ext} \sin\varphi \end{pmatrix}. \quad (27)$$

By definition, the electric field is tangent to any field line, so $\vec{E} = K_0(s)\vec{\tau}$, where $\vec{\tau}$ is the unitary vector tangent to a field line in s :

$$\vec{\tau} = \frac{d\vec{r}}{ds} = \begin{pmatrix} \frac{dr}{ds} \\ r \frac{d\varphi}{ds} \end{pmatrix}. \quad (28)$$

Equalising both expressions of the electric field we get:

$$\frac{q}{4\pi\epsilon r^2} + E_{ext} \cos\varphi = K_0(s) \frac{dr}{ds}. \quad (29)$$

$$-E_{ext} \sin\varphi = K_0(s) r \frac{d\varphi}{ds}. \quad (30)$$

Then, from Eq. 30 we isolate ds , $ds = -\frac{K_0(s)r}{E_{ext}\sin\varphi}d\varphi$, and we substitute this expression in Eq. 29 to obtain

$$\frac{q}{4\pi\epsilon r^2} + E_{ext} \cos\varphi = -E_{ext} \sin\varphi \frac{1}{r} \frac{dr}{d\varphi}. \quad (31)$$

We multiply Eq. 31 by r^2/E_{ext} , getting

$$\frac{q}{4\pi\epsilon E_{ext}} + r^2 \cos\varphi = -\sin\varphi r \frac{dr}{d\varphi}. \quad (32)$$

We perform the change of variable $h = r^2$, $dh = 2rdr$ in Eq. 32 and we also define $K_1 = q/4\pi\epsilon E_{ext}$, thus

$$\begin{aligned} K_1 + h\cos\varphi &= -\frac{\sin\varphi}{2} \frac{dh}{d\varphi}, \\ \frac{dh}{d\varphi} + \frac{2h}{\tan\varphi} &= -\frac{2K_1}{\sin\varphi}, \end{aligned} \quad (33)$$

which is a first order differential equation. The integration factor is:

$$F(\varphi) = \exp\left(\int \frac{2}{\tan x} dx\right) = \exp\left(\int \frac{2\cos x}{\sin x} dx\right) = \exp(2 \ln(\sin\varphi)) = \sin^2\varphi, \quad (34)$$

and the solution of Eq. 33 is given by

$$h = -\frac{1}{F(\varphi)} \int F(x) \frac{2K_1}{\sin x} dx = -\frac{2K_1}{\sin^2\varphi} \int \sin x dx = -\frac{2K_1}{\sin^2\varphi} (-\cos\varphi + C). \quad (35)$$

As a result, the expression of the field lines, considering the previous change of variable, $h = r^2$, is the following:

$$r(\varphi) = \sqrt{h} = \sqrt{\frac{-q}{2\pi\epsilon E_{ext}}} \frac{\sqrt{C - \cos\varphi}}{\sin\varphi}. \quad (36)$$

Eq. 36 defines the field according with the parameter C (see Fig. 2). Considering an external electric field of 1 kV/cm, the value of the scale factor $\sqrt{-q/2\pi\epsilon E_{ext}}$ is 0.14 μm . Depending on the value of the parameter C , we distinguish four different cases:

1. If $C > 1$, $r(\varphi)$ is defined in the whole interval $(0, \pi)$ of φ . Since $r(\varphi) \rightarrow \infty$ when φ approaches to the limits of the interval, the equation represents a line that goes from $-\infty$ to ∞ .
2. If $-1 < C < 1$, there are values of φ near to 0 for which $r(\varphi)$ is not defined. Since the value of $r(\varphi)$ for the minimum of φ is zero, the equation represents a line that goes from $-\infty$ to the origin.
3. If $C < -1$, $r(\varphi)$ is not defined.

The flux tube that includes all the field lines that end in the ion is defined by $C = 1$, and the value of the transverse section of the flux tube with $C = 1$ in a point far from the ion is:

$$\pi r_y^2(\varphi \rightarrow \pi) = \pi r^2 \sin^2\varphi = \pi \frac{-q}{2\pi\epsilon E_{ext}} (1 - \cos\varphi) \simeq \frac{-q}{\epsilon E_{ext}}. \quad (37)$$

Fig. 2 shows the field lines approaching the ion, positioned at (0,0) which has a negligible size at the micron scale. The lines correspond to different values of C , at the same time the red line ($C = 1$) gives the envelope of all the field lines ending on the ion.

B. CATHODE VOLTAGE CALCULATION

The cathode voltage necessary to obtain a given field taking into account the ion current can be calculated integrating the drift field expression given by Eq. 20 along the drift path.

$$V(L) = \int_0^L E_d(l) dl = \sqrt{\frac{hq}{\epsilon\mu_i}} \int_0^L \sqrt{l^2 + 2\frac{j_i(0)}{h}l + \frac{f_0}{h}} dl. \quad (38)$$

Defining for simplicity $s = l + j_i(0)/h$ and $R = \sqrt{f_0/h - (j_i(0)/h)^2}$ we can get

$$\begin{aligned} V(L) &= \sqrt{\frac{hq}{\epsilon\mu_i}} \int_{j_i(0)/h}^{L+j_i(0)/h} \sqrt{s^2 + R^2} ds \\ &= \frac{1}{2} \sqrt{\frac{hq}{\epsilon\mu_i}} \left[s\sqrt{s^2 + R^2} + R^2 \ln \left(s + \sqrt{s^2 + R^2} \right) \right]_{j_i(0)/h}^{L+j_i(0)/h}. \end{aligned} \quad (39)$$

Substituting the integration limits we finally have

$$\begin{aligned} V(L) &= \frac{1}{2} \sqrt{\frac{hq}{\epsilon\mu_i}} \left[\left(L + \frac{j_i(0)}{h} \right) \sqrt{\left(L + \frac{j_i(0)}{h} \right)^2 + R^2} \right. \\ &\quad + R^2 \ln \left(L + \frac{j_i(0)}{h} + \sqrt{\left(L + \frac{j_i(0)}{h} \right)^2 + R^2} \right) - \frac{j_i(0)}{h} \sqrt{\frac{f_0}{h}} \\ &\quad \left. - R^2 \ln \left(\frac{j_i(0)}{h} + \sqrt{\frac{f_0}{h}} \right) \right], \end{aligned} \quad (40)$$

which expresses the cathode voltage as function of the constant ionization rate h and the ion current at the anode $j_i(0)$ for a detector with a given drift length L .

- [1] C. Rubbia *et al.*, “Underground operation of the ICARUS T600 LAr-TPC: first results,” *JINST* **6** (2011) P07011 [arXiv:1106.0975 [hep-ex]].
- [2] C. Anderson *et al.* [ArgoNeuT Collaboration], “Analysis of a Large Sample of Neutrino-Induced Muons with the ArgoNeuT Detector,” *JINST* **7** (2012) P10020 [arXiv:1205.6702 [physics.ins-det]].

- [3] C. M. Ignarra [MicroBooNE Collaboration], “MicroBooNE,” arXiv:1110.1604 [physics.ins-det].
- [4] P. Benetti *et al.*, “First results from a Dark Matter search with liquid Argon at 87 K in the Gran Sasso Underground Laboratory,” *Astropart. Phys.* **28** (2008) 495 [astro-ph/0701286].
- [5] A. Badertscher *et al.*, “ArDM: first results from underground commissioning,” *JINST* **8** (2013) C09005 [arXiv:1309.3992 [physics.ins-det]].
- [6] P. Agnes *et al.* [DarkSide Collaboration], “First Results from the DarkSide-50 Dark Matter Experiment at Laboratori Nazionali del Gran Sasso,” *Phys. Lett. B* **743** (2015) 456 [arXiv:1410.0653 [astro-ph.CO]].
- [7] C. Adams *et al.* [LBNE Collaboration], “The Long-Baseline Neutrino Experiment: Exploring Fundamental Symmetries of the Universe,” FERMILAB-PUB-14-022, arXiv:1307.7335 [hep-ex].
- [8] V. Chepel and H. Araujo, “Liquid noble gas detectors for low energy particle physics,” *JINST* **8** (2013) R04001 [arXiv:1207.2292 [physics.ins-det]].
- [9] S. Amerio *et al.* [ICARUS Collaboration], “Design, construction and tests of the ICARUS T600 detector,” *Nucl. Instrum. Meth. A* **527** (2004) 329.
- [10] A. Rubbia [WA105 Collaboration], “Technical Design Report for large-scale neutrino detectors prototyping and phased performance assessment in view of a long-baseline oscillation experiment,” CERN-SPSC-2014-013.
- [11] S. Murphy [LAGUNA-LBNO Collaboration], “GLACIER for LBNO: Physics Motivation and R&D Results,” *Phys. Procedia* **61** (2015) 560.
- [12] D. B. Cline, F. Raffaelli and F. Sergiampietri, “LANNDD: A line of liquid argon TPC detectors scalable in mass from 200 Tons to 100 Ktons,” *JINST* **1** (2006) T09001 [astro-ph/0604548].
- [13] D. Angeli *et al.*, “Towards a new Liquid Argon Imaging Chamber for the MODULAr project,” *JINST* **4** (2009) P02003.
- [14] L. Agostino *et al.*, “LBNO-DEMO: Large-scale neutrino detector demonstrators for phased performance assessment in view of a long-baseline oscillation experiment,” arXiv:1409.4405 [physics.ins-det].
- [15] T. Tope *et al.*, “Extreme argon purity in a large, non-evacuated cryostat,” *AIP Conf. Proc.* 1573, 1169 (2014).

- [16] E. Buckley *et al.*, “A study of ionization electrons drifting over large distances in liquid argon,” Nuclear Instruments and Methods in Physics Research A 275, 364 (1989).
- [17] W. Walkowiak, “Drift velocity of free electrons in liquid argon,” Nucl. Instrum. Meth. A **449** (2000) 288.
- [18] T.H. Dey, T.J. Lewis “Ion mobility and liquid motion in liquefied argon,” J. Phys. D: Applied Physics, vol. 1, n 8, p 1019, (1968).
- [19] D. J. Griffiths, “Introduction to Electrodynamics”, Ed. Pearson, 2013 (4th edition), pag. 121. ISBN: 0321856562.
- [20] L. Bruschi, G. Mazzi, M. Santini, and G. Torzo, “Transmission of negative ions through the liquid-vapor surface in neon”, J. Phys. C: Solid State Phys., Vol. 8 (1975), 1412
- [21] A.F. Borghesani, G. Carugno, M. Cavenago, and E. Conti, “Electron transmission through the Ar liquid-vapor interface”, Phys. Lett. A149 (1990), 481.
- [22] A. Bueno, Z. Dai, Y. Ge, M. Laffranchi, A. J. Melgarejo, A. Meregaglia, S. Navas and A. Rubbia, “Nucleon decay searches with large liquid argon TPC detectors at shallow depths: Atmospheric neutrinos and cosmogenic backgrounds’, JHEP **0704** (2007) 041 [hep-ph/0701101].
- [23] M. Torti “Search for space charge effects in the ICARUS T600 LAR-TPC”, Poster at the 4th International Conference on New Frontiers in Physics (2015)
- [24] P. Benetti *et al.* [WARP Collaboration], “Measurement of the specific activity of Ar-39 in natural argon’, Nucl. Instrum. Meth. A **574** (2007) 83 [astro-ph/0603131].
- [25] M. Miyajima, *et al.*, “Average energy expended per ion pair in liquid argon”, Phys. Rev. A 9 (1974) 1438
- [26] J. Birks, “Theory and Practice of Scintillation Counting”, Pergamon Press, New York, 1964
- [27] R.T. Scalettar *et al.*, “Critical test of geminate recombination in liquid argon”, Phys. Rev. A 25 (1982) 2419.
- [28] P. K. F. Grieder, “Cosmic rays at earth: Researcher’s reference, manual and data book”, Amsterdam: Elsevier (2001), ISBN: 9780444507105.
- [29] A. Ereditato *et al.*, “Measurement of the drift field in the ARGONTUBE LAr TPC with 266 nm pulsed laser beams”, JINST **9** (2014) no.11, P11010
- [30] M. Mooney, “The MicroBooNE Experiment and the Impact of Space Charge Effects”, arXiv:1511.01563 [physics.ins-det].

[31] R. Acciarri *et al.*, “Long-Baseline Neutrino Facility (LBNF) and Deep Underground Neutrino Experiment (DUNE) Conceptual Design Report Volume 1: The LBNF and DUNE Projects”, arXiv:1601.05471 [physics.ins-det].